Scientia Iranica B (2014) 21(3), 578–586

SCIENTIA IRANICA

Sharif University of Technology
Scientia Iranica
Transactions B: Mechanical Engineering
www.scientiairanica.com

Viscoelastic potential flow analysis of the stability of a cylindrical jet

M.K. Awasthi[a*], R. Asthana[b] and G.S. Agrawal[c]

a. *Department of Mathematics, University of Petroleum and Energy Studies, Dehradun, 248007, India.*
b. *Department of Mathematics, Galgotia University, Greater Noida, 201306, India.*
c. *Institute of Computer Application, Manglayatan University, Aligarh, 202145, India.*

Received 17 April 2012; received in revised form 12 September 2013; accepted 15 October 2013

KEYWORDS
Viscoelastic potential flow;
Cylindrical jet;
Maxwell type fluid;
Interfacial flows;
Viscous stresses.

Abstract. A linear analysis of the temporal instability of a viscoelastic liquid jet with axisymmetric and asymmetric disturbances moving in an infinite viscous fluid is investigated. The cause of the instability in the liquid jet is Kelvin-Helmholtz instability, due to the velocity difference and capillary instability, due to surface tension. The dispersion relation for viscoelastic potential flow is cubic in nature. The stability analysis shows that viscoelastic liquid jets are less unstable than inviscid jets and more unstable than viscous liquid jets for both axisymmetric and asymmetric disturbances. Stability analysis has been undertaken in terms of various parameters, such as Weber number, Reynolds number, Deborah number etc.

1. Introduction

Breakup of liquid jet into drops is a natural phenomenon. It has many practical applications such as in gas turbine engines, oil burners and lubrication etc. Since, in many of these processes, non-Newtonian liquids may be involved, it is of interest and importance to understand the mechanisms of instability of such liquids.

Capillary instability arises when a liquid cylinder in an infinite fluid collapses under the action of capillary forces due to surface tension. The capillary instability of a liquid jet of radius R under the action of capillary force was studied by Rayleigh [1]. The analysis of Rayleigh was based on potential flow of an inviscid liquid, neglecting the effect of outside fluid. He observed that the jet is unstable to all axisymmetric disturbances having wavelengths greater than $2\pi R$. Chandrasekhar [2] extended this problem to nonaxisymmetric disturbances and observed that liquid jet is always stable for non-axisymmetric modes. He also observed that if the fluid is bounded by two cylindrical interfaces with radii $R_1, R_2 (R_1 < R_2)$, then the fluid is stable if both are kR_1, kR_2 (k is the wave number) are greater than unity, and thus, Rayleigh's criterion for a single interface is still true for two cylindrical interfaces. Rayleigh [3] again established the result for viscous effect, neglecting surrounding fluids. The effect of viscosity, with the assumption that at high viscosity inertia is neglected, the wavelength for maximum growth rate is very large, strictly infinity. Weber [4] made another extension to Rayleigh's theory by considering the effect of viscosity and surrounding air on the stability of the columnar jet.

The linear stability analysis of the capillary instability of a viscoelastic fluid was done by Middleman [5] and Goldin et al. [6], and they observed that growth rates are larger for viscoelastic fluid. Later, Chang et al. [7] and Bousfield et al. [8] investigated the capillary instability for viscoelastic fluids. Brenn et

*. *Corresponding author. Tel.: +91 1332285157; Fax: +91 133273560*
E-mail addresses: mukeshiitr.kumar@gmail.com (M.K. Awasthi); rasthana4@gmail.com (R. Asthana); gsa45fma@gmail.com (G.S. Agrawal)

al. [9] studied the linear temporal instability of an axisymmetrical non-Newtonian liquid jet. Liu and Liu [10] undertook the linear analysis of the three-dimensional instability of non-Newtonian liquid jets. The instability of a viscoelastic liquid jet with axisymmetric and asymmetric disturbances has been studied by Liu and Liu [11]. They concluded that at small Weber number, axisymmetric disturbance dominates the instability of viscoelastic jets.

In Viscous Potential Flow (VPF) theory, the viscous term in the Navier-stokes equation is identically zero when the vorticity is zero, but the viscous stresses are not zero [12]. Tangential stresses are not considered in VPF theory and viscosity enters through normal stress balance. In this theory, the no-slip condition at the boundary is not enforced, so that two dimensional solutions satisfy three dimensional solutions. Kelvin-Helmholtz instability occurs when there is a relative motion between the fluid layers of different physical parameters. The VPF analysis of Kelvin-Helmholtz instability was studied by Funada and Joseph [13]. They have observed that the stability criterion for viscous potential flow is given by the critical value of relative velocity. The instability of the plane interface separating two fluids having different densities, when the lighter fluid is accelerated toward the heavier fluid, is called Rayleigh-Taylor instability. Joseph et al. [14] have studied VPF analysis of Rayleigh-Taylor instability. Joseph et al. [15] have done Rayleigh-Taylor instability of viscoelastic drops at high Weber numbers and concluded that the most unstable wave is a sensitive function of the retardation time, λ_2, which fits experiments when $\lambda_2/\lambda_1 = O(10^{-3})$. The viscous potential flow analysis of capillary instability has been studied by Funada and Joseph [16]. They observed that viscous potential flow is a better approximation of the exact solution than the inviscid model. Funada and Joseph [17] extended their study of capillary instability to the viscoelastic fluids of Maxwell type and observed that the growth rates are larger for viscoelastic fluids than for the equivalent Newtonian fluids. The stability of liquid jet into incompressible gases and liquids was computed by Funada et al. [18]. They consider both Kelvin-Helmholtz and capillary instabilities and observed that Kelvin-Helmholtz instability cannot occur in a vacuum but capillary instability.

The objective of the present work is to investigate the mechanism of the temporal instability of a viscoelastic liquid jet moving in an infinite viscous fluid with both axisymmetric and asymmetric disturbances using potential flow theory. The inside fluid is taken as the viscoelastic fluid of Oldroyd-B type and the outside fluid as a viscous fluid. Liquid jet instability is associated with Kelvin-Helmholtz instability, as well as capillary instability, and, therefore, we consider both instabilities in the present analysis. The dispersion relation for the viscoelastic potential flow is derived, and the effect of various parameters on the instability behaviour is examined. The variation of growth rates with Deborah number, which depends linearly on relaxation time, is observed. The dispersion relation of Funada et al. [18] has been reduced by our relation. A number of conclusions have been made on the instability behaviour of viscoelastic jets for both asymmetric and axisymmetric disturbances.

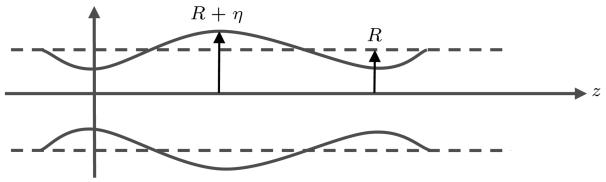

Figure 1. The perturbed jet. The coordinate system is fixed to moving jet.

2. Problem formulation

Consider a cylindrical jet of viscoelastic fluid, with density $\rho^{(1)}$, viscosity $\mu^{(1)}$ and mean radius R, moving with a uniform axial velocity, U, in an infinite viscous fluid of density, $\rho^{(2)}$, viscosity, $\mu^{(2)}$, with a cylindrical reference frame (r, θ, z), as seen in Figure 1. The fluid cylinder is lying in the region of $0 \leq r < R + \eta$ and $-\infty < z < \infty$ where $\eta = \eta(\theta, z, t)$ is the interface displacement. Surface tension at the interface is taken as. Both the fluid flows are assumed to be incompressible and irrotational.

Viscoelastic fluids are basically non-Newtonian fluids that can exhibit a response that resembles that of an elastic solid under some circumstances, or the response of a viscous liquid under others. The viscoelastic fluid considered in this analysis is of the Oldroyd-B type [17], because it has a feature that combines the effects of relaxation and nonlinearity, with a relative case of execution, better than any other viscoelastic fluid. The constitutive equation of the linear viscoelastic fluid of Oldroyed-B type is given by:

$$\left[1 + \lambda_1 \frac{\partial}{\partial t}\right] \tau = 2\mu^{(1)} \left[1 + \lambda_2 \frac{\partial}{\partial t}\right] \gamma, \tag{1}$$

where τ is the viscous stress tensor, $\mu^{(1)}$ is the viscosity, γ is the strain tensor and λ_1 and λ_2 are the relaxation and retardation times, respectively.

Small disturbances are imposed onto the equilibrium state. After disturbance, the interface is given by:

$$F(r, \theta, z, t) = r - R - \eta(\theta, z, t) = 0, \tag{2}$$

where η is the perturbation in the radius of the interface from the equilibrium value, R, and for which the unit

outward normal is given by:

$$n = \left\{1 + \left(\frac{1}{r}\frac{\partial \eta}{\partial \theta}\right)^2 + \left(\frac{\partial \eta}{\partial z}\right)^2\right\}^{-1.2} \left(e_r - \frac{1}{r}\frac{\partial \eta}{\partial \theta}e_\theta - \frac{\partial \eta}{\partial z}e_z\right), \quad (3)$$

where e_r, e_θ and e_z, are unit vectors along the r, θ and z directions, respectively.

The velocity is expressed as the gradient of a potential function and the potential functions satisfy the Laplace equation, as a consequence of the incompressibility constraint, i.e:

$$\nabla^2 \phi^{(j)} = 0 \quad (j = 1, 2), \quad (4)$$

where:

$$\nabla^2 = \frac{\partial^2}{\partial r^2} + \frac{1}{r}\frac{\partial}{\partial r} + \frac{1}{r^2}\frac{\partial^2}{\partial \theta^2} + \frac{\partial^2}{\partial z^2}.$$

As per the kinematic condition, every particle on the interface will remain on the interface. Thus, we get the following boundary conditions:

$$\frac{\partial \eta}{\partial t} + U\frac{\partial \eta}{\partial z} = \frac{\partial \phi^{(1)}}{\partial r} \quad \text{at} \quad r = R, \quad (5)$$

$$\frac{\partial \eta}{\partial t} = \frac{\partial \phi^{(2)}}{\partial r} \quad \text{at} \quad r = R. \quad (6)$$

Using a normal mode technique to solve Eq. (4), we can get:

$$\phi^{(j)} = [A^{(j)} I_n(kr) + B^{(j)} K_n(kr)] \exp(ikz + in\theta - i\omega t) + c.c., \quad (7)$$

where $I_n(kr)$ and $K_n(kr)$ Bessel's function of first and second kind of order n, respectively, and *c.c.* denotes the complex conjugate of the preceding term.

For viscoelastic fluid (inside fluid), the potential function, ϕ, is finite at $r \to 0$, so $B^{(1)} = 0$ and for viscous fluid (outside fluid), ϕ is finite at $r \to \infty$, so, $A^{(2)} = 0$. Hence:

$$\phi^{(1)} = A^{(1)} I_n(kr) \exp(ikz + in\theta - i\omega t) + c.c. , \quad (8)$$

$$\phi^{(2)} = B^{(2)} K_n(kr) \exp(ikz + in\theta - i\omega t) + c.c. \quad (9)$$

The interface elevation is given by:

$$\eta = C \exp(ikz + in\theta - i\omega t) + c.c., \quad (10)$$

where C denotes complex constant, k is the real wave number and ω represents the growth rate.

Using the kinematic conditions (Eqs. (5) and (6)), we get the following solution for $\phi^{(1)}$ and $\phi^{(2)}$:

$$\phi^{(1)} = (ikU + i\omega) C E^{(1)}(kr) \exp(ikz + in\theta - i\omega t) + c.c., \quad (11)$$

$$\phi^{(2)} = -i\omega C E^{(2)}(kr) \exp(ikz + in\theta - i\omega t) + c.c., \quad (12)$$

where:

$$E^{(1)}(kr) = \frac{I_n(kr)}{I'_n(kR)}, \quad E^{(2)}(kr) = \frac{K_n(kr)}{K'_n(kR)}.$$

3. Dispersion relation

The dynamical condition, wherein the normal stresses should be continuous across the interface, is given by:

$$p_1 - p_2 - 2\mu^{(1)}\frac{\partial^2 \phi^{(1)}}{\partial r^2} + 2\mu^{(2)}\frac{\partial^2 \phi^{(2)}}{\partial r^2} = -\sigma\left(\frac{\partial^2 \eta}{\partial z^2} + \frac{1}{r^2}\frac{\partial^2 \eta}{\partial \theta^2} + \frac{\eta}{R^2}\right), \quad (13)$$

where $p_j (j = 1, 2)$ is the pressure for the inside and outside fluids, respectively, and σ represents the surface tension. Using Bernoulli's equation for irrotational pressure and linearizing it, we get:

$$-\rho^{(1)}\left(\frac{\partial \phi^{(1)}}{\partial t} + U\frac{\partial \phi^{(1)}}{\partial z}\right) + \rho^{(2)}\left(\frac{\partial \phi^{(2)}}{\partial t}\right) - 2\mu^{(1)}\frac{\partial^2 \phi^{(1)}}{\partial r^2} + 2\mu^{(1)}\frac{\partial^2 \phi^{(2)}}{\partial r^2} = -\sigma\left(\frac{\partial^2 \eta}{\partial z^2} + \frac{1}{r^2}\frac{\partial^2 \eta}{\partial \theta^2} + \frac{\eta}{R^2}\right). \quad (14)$$

Substituting the values of $\eta, \phi^{(1)}$ and $\phi^{(2)}$ in Eq. (14), we get the relation:

$$\rho^{(1)}(\omega - kU)^2 E^{(1)}(kR) - \omega^2 \rho^{(2)} E^{(2)}(kR) - 2i\mu^{(1)}k^2(kU - \omega)F^{(1)}(kR) - 2i\mu^{(2)}k^2\omega F^{(2)}(kR) = \sigma\left(k^2 + \frac{n^2 - 1}{R^2}\right), \quad (15)$$

where:

$$F^{(1)}(kR) = \frac{I''_n(kR)}{I'_n(kR)} - \left(1 + \frac{n^2}{k^2R^2}\right)E^{(1)}(kR) - \frac{1}{kR},$$

$$F^{(2)}(kR) = \frac{K''_n(kR)}{K'_n(kR)} - \left(1 + \frac{n^2}{k^2R^2}\right)E^{(2)}(kR) - \frac{1}{kR}.$$

Since the inside fluid is the viscoelastic fluid of the

Olroyed-B type, the viscosity, $\mu^{(1)}$, is modified as $\frac{1-i\lambda_2\omega}{1-i\lambda_1\omega}\mu^{(1)}$. Hence, the dispersion relation for the VPF analysis is given by:

$$a_3\omega^3 + (a_2 + ib_2)\omega^2 + (a_1 + ib_1)\omega + (a_0 + ib_0) = 0, \tag{16}$$

where:

$$a_3 = \lambda_1(\rho^{(1)}E^{(1)}(kR) - \rho^{(2)}E^{(2)}(kR)),$$

$$a_2 = -2k\lambda_1 U\rho^{(1)}E^{(1)}(kR),$$

$$b_2 = (\rho^{(1)}E^{(1)}(kR) - \rho^{(2)}E^{(2)}(kR)) + 2k^2(\lambda_2\mu^{(1)}F^{(1)}(kR) - \lambda_1\mu^{(2)}F^{(2)}(kR)),$$

$$a_1 = \lambda_1\left(k^2U^2\rho^{(1)}E^{(1)}(kR) - \sigma k(k^2 + \frac{n^2-1}{R^2})\right) - 2k^2(\mu^{(1)}F^{(1)}(kR) - \mu^{(2)}F^{(2)}(kR)),$$

$$b_1 = -2kU\rho^{(1)}E^{(1)}(kR) - 2k^3U\lambda_2\mu^{(1)}F^{(1)}(kR),$$

$$a_0 = 2k^3U\mu^{(1)}F^{(1)}(kR),$$

$$b_0 = k^2U^2\rho^{(1)}E^{(1)}(kR) - \sigma k(k^2 + \frac{n^2-1}{R^2}).$$

In case of axisymmetric disturbances ($n = 0$), the dispersion relation becomes:

$$\begin{aligned}[\lambda_1(\rho^{(1)}\alpha_1 + \rho^{(2)}\alpha_2)]\omega^3 + [&-2k\lambda_1U\rho^{(1)}\alpha_1 \\ &+ i(\rho^{(1)}\alpha_1 + \rho^{(2)}\alpha_2 + 2k^2(\lambda_2\mu^{(1)}\beta_1 \\ &+ \lambda_1\mu^{(2)}\beta_2))]\omega^2 + \left[\lambda_1\left(k^2U^2\rho^{(1)}\alpha_1\right.\right. \\ &\left.\left. - \sigma k(k^2 - \frac{1}{R^2})\right) - 2k^2(\mu^{(1)}\beta_1 + \mu^{(2)}\beta_2)\right. \\ &\left. + i(-2kU\rho^{(1)}\alpha_1 - 2k^3U\lambda_2\mu^{(1)}\beta_1)\right]\omega \\ &+ \left[2k^3U\mu^{(1)}\beta_1 + i\left(b_0 = k^2U^2\rho^{(1)}\alpha_1\right.\right. \\ &\left.\left. - \sigma k(k^2 - \frac{1}{R^2})\right)\right] = 0, \end{aligned} \tag{17}$$

where:

$$\alpha_1 = \frac{I_0(kR)}{I_1(kR)}, \qquad \beta_1 = \alpha_1 - \frac{1}{kR},$$

$$\alpha_2 = \frac{K_0(kR)}{K_1(kR)}, \qquad \beta_1 = \alpha_1 - \frac{1}{kR}.$$

If both fluids are viscous, i.e. $\lambda_1 = \lambda_2$, the dispersion relation (17) reduces the same expression as obtained by Funada et al. [18]. If we put $U = 0$ and $\omega = i\omega$ in Eq. (17), the dispersion relation reduces to the dispersion relation, which is the dimensional form of the dispersion relation obtained by Funada and Joseph [17]. If we put $\lambda_1 = \lambda_2$, again, the dispersion relation reduces to the dimensional form of the same dispersion relation, as obtained by Funada and Joseph [16].

4. Non-dimensional form

Consider the non-dimensional variables:

$$D = 2R, \qquad \Lambda_1 = \frac{\lambda_1 V}{D}, \qquad \Lambda_2 = \frac{\lambda_2 V}{D},$$

$$\hat{\omega} = \frac{\omega D}{V}, \qquad \hat{\rho} = \frac{\rho^{(2)}}{\rho^{(1)}}, \qquad \hat{\mu} = \frac{\mu^{(2)}}{\mu^{(1)}},$$

$$\hat{R} = \frac{R}{D} = \frac{1}{2}, \qquad \hat{k} = kD, \qquad \mathrm{Re} = \frac{\rho^{(1)}}{\mu^{(1)}},$$

$$W = \frac{\rho^{(1)}DV^2}{\sigma}, \qquad \hat{U} = \frac{U}{V},$$

where Re denotes the Reynolds number, which is defined as the ratio of inertia forces to viscous forces. The ratio of the inertia force to the surface tension force is known as the Weber number denoted by W, and Λ_1, Λ_2 are known as Deborah number. $\hat{\rho}$ and $\hat{\mu}$ are the density and viscosity ratios, respectively.

The dimensionless form of the dispersion relation for the VPF analysis (16) is given by:

$$\hat{a}_3\hat{\omega}^3 + (\hat{a}_2 + i\hat{b}_2)\hat{\omega}^2 + (\hat{a}_1 + i\hat{b}_1)\hat{\omega} + (\hat{a}_0 + i\hat{b}_0) = 0, \tag{18}$$

where:

$$\hat{a}_3 = \Lambda_1(E^{(1)}(\hat{k}/2) - \hat{\rho}E^{(2)}(\hat{k}/2)),$$

$$\hat{a}_2 = -2\hat{k}\hat{U}\Lambda_1E^{(1)}(\hat{k}/2),$$

$$\hat{b}_2 = (E^{(1)}(\hat{k}/2) - \hat{\rho}E^{(2)}(\hat{k}/2)) + \frac{2\hat{k}^2}{\mathrm{Re}}(\Lambda_2F^{(1)}(\hat{k}/2) - \Lambda_1\hat{\mu}F^{(2)}(\hat{k}/2)),$$

$$\hat{a}_1 = \Lambda_1\left(\hat{k}^2\hat{U}^2E^{(1)}(\hat{k}/2) - W^{-1}\hat{k}(\hat{k}^2 + 4(n^2-1))\right) - \frac{2\hat{k}^2}{\mathrm{Re}}\left(F^{(1)}(\hat{k}/2) - \hat{\mu}F^{(2)}(\hat{k}/2)\right),$$

$$\hat{b}_1 = -2\hat{k}\hat{U}E^{(1)}(\hat{k}/2) - \Lambda_2\frac{2\hat{k}^3}{\mathrm{Re}}\hat{U}F^{(1)}(\hat{k}/2),$$

$$\hat{a}_0 = \frac{2\hat{k}^3}{\mathrm{Re}}\hat{U}F^{(1)}(\hat{k}/2),$$

$$\hat{b}_0 = \hat{k}^2\hat{U}^2E^{(1)}(\hat{k}/2) - W^{-1}\hat{k}(\hat{k}^2 + 4(n^2-1)).$$

For axisymmetric disturbances, i.e for $n = 0$:

$$A_0(\hat{k}/2) = \frac{I_0(\hat{k}/2)}{I_1(\hat{k}/2)} = \alpha_1,$$

$$B_0(\hat{k}/2) = -\frac{K_0(\hat{k}/2)}{K_1(\hat{k}/2)} = -\alpha_a,$$

$$A_t(\hat{k}/2) = \frac{I_0''(\hat{k}/2)}{I_0'(\hat{k}/2)} = \alpha_1 - \frac{2}{\hat{k}} = \beta_l,$$

$$B_t(\hat{k}/2) = \frac{K_0''(\hat{k}/2)}{K_0'(\hat{k}/2)} = -\left(\alpha_a + \frac{2}{\hat{k}}\right) = -\beta_a.$$

Hence, the dispersion relation for the axisymmetric case is:

$$[\Lambda_1(\alpha_1 + \hat{\rho}\alpha_a)]\hat{\omega}^3 + \Bigg[-2\hat{k}\hat{U}\Lambda_1\alpha_1 + i\Bigg((\alpha_l + \hat{\rho}\alpha_a) + \frac{2\hat{k}^2}{\mathrm{Re}}(\Lambda_2\beta_l + \lambda_1\hat{\mu}\beta_a)\Bigg)\Bigg]\hat{\omega}^2 + \Bigg[\Lambda_1(\hat{k}^2\hat{U}^2\alpha_l - \mathrm{W}^{-1}\hat{k}(\hat{k}^2-4))\Bigg] - \frac{2k^2}{\mathrm{Re}}(\beta_l + \hat{\mu}\beta_a) - 2i\hat{k}\hat{U}\alpha_l - i\frac{2\hat{k}^3}{\mathrm{Re}}\Lambda_2\hat{U}\beta_l\Bigg]\hat{\omega} + \Bigg[\frac{2k^3}{\mathrm{Re}}\hat{U}\beta_1 + i(\hat{k}^2\hat{U}^2\alpha_l - \mathrm{W}^{-1}\hat{k}(\hat{k}^2-4)) + \Bigg] = 0. \quad (19)$$

If we put Deborah number $\Lambda_1 = \Lambda_2$ and $\hat{U} = 1$ in Eq. (19), the dispersion relation becomes:

$$(\alpha_l + \hat{\rho}\alpha_a)\hat{\omega}^2 + \left[-2\hat{k}\alpha_l + i\frac{2\hat{k}^2}{\mathrm{Re}}(\beta_l + \hat{\mu}\beta_a)\right]\hat{\omega} + \left[\hat{k}^2\alpha_l - i\frac{2k^3}{\mathrm{Re}}\beta_l - W^{-1}\hat{k}(\hat{k}^2 - 4\hat{k})\right] = 0. \quad (20)$$

This is the same dispersion relation as obtained by Funada et al. [18]. For inviscid liquid jet, i.e Re$\rightarrow\infty$ and $\hat{\mu} = 0$, the dispersion relation for the inviscid jet is given by:

$$(\alpha_l + \hat{\rho}\alpha_a)\hat{\omega}^2 + [-2\hat{k}\alpha_l]\hat{\omega} + [\hat{k}^2\alpha_l - W^{-1}\hat{k}(\hat{k}^2-4)] = 0. \quad (21)$$

If there is no surface tension at the interface, i.e. $\sigma = 0$ and the jet is inviscid, so W$\rightarrow\infty$ and Re $\rightarrow\infty$, the dispersion relation for an axisymmetric jet can be written as:

$$[\Lambda_1(\alpha_l + \hat{\rho}\alpha_a)]\hat{\omega}^3 + [-2\hat{k}\hat{U}\Lambda_1\alpha_l + i(\alpha_l + \hat{\rho}\alpha_a)]\hat{\omega}^2[\Lambda_1\hat{k}^2\hat{U}^2\alpha_l - 2i\hat{k}\hat{U}\alpha_l]\hat{\omega} + [i(\hat{k}^2\hat{U}^2\alpha_l)] = 0. \quad (22)$$

5. Results and discussions

The dispersion relation for viscoelastic jets is cubic in nature and instability occurs due to the positive values of the disturbance growth rate (i.e. $\omega_I > 0$). If ω_I is negative, the perturbation decays with time, while, if $\omega_I > 0$, the system is unstable, as the perturbation grows exponentially with time. Case $\omega_I = 0$ is a marginal stability case. The viscoelastic fluid properties and the parameters used are given in Table 1 [17].

Funada et al. [18] have pointed out that the cause of the instability in the liquid jet is Kelvin-Helmholtz instability due to the velocity difference, and capillary instability due to surface tension. For Weber number W $\rightarrow\infty$, the effect of surface tension vanishes, so, the instability in the liquid jet becomes pure Kelvin-Helmholtz instability. If the Weber number is W = 0, the instability in the liquid jet is driven by pure capillary instability.

In Figures 2-8, the growth rate curves have been plotted for the axisymmetric disturbances. Figure 2 shows the comparison between the maximum growth rate curves for inviscid liquid jet, viscous liquid jet and the cylindrical jet of viscoelastic fluid. Here, the viscoelastic fluid of Maxwell type (2% Poly Acrylic Acid, PAA) has been taken. Maximum growth rate curves plotted here for viscous and inviscid jets are

Table 1. Viscoelastic fluid properties and parameters.

	2% PAA	**2% PO**
$\rho^{(1)}$ (gcm^{-3})	0.99	0.99
$\mu^{(1)}(P)$	96.0	350.0
$\rho^{(2)}$ (gcm^{-3})	1.947×10^{-3}	1.776×10^{-3}
$\mu^{(2)}(P)$	1.8×10^{-4}	1.8×10^{-4}
σ(dyn cm^{-1})	45.0	63.0
λ_1 (s)	0.039	0.21
λ_2 (s)	0.0	0.0
V(cm s^{-1})	0.4688	0.18
Re	206.8466	1964.10
W	206.8246	1964.10
$\hat{\rho}$	1.967×10^{-3}	1.794×10^{-3}
$\hat{\mu}$	1.875×10^{-6}	5.143×10^{-7}
Λ_1	0.01828	0.0378
Λ_2	0.0	0.0

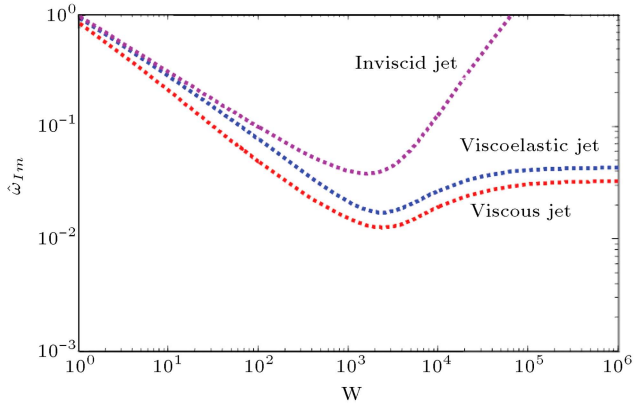

Figure 2. The maximum growth rates $\hat{\omega}_{Im}$ versus Weber number, W, for inviscid jet, viscous jet and viscoelastic jet (2%PAA) with $\hat{U} = 1$ and Re = 100.

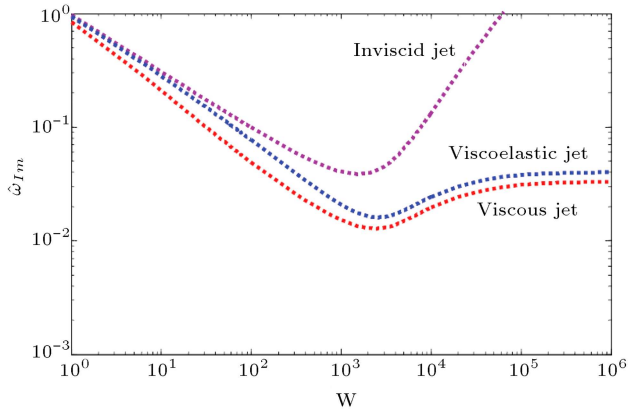

Figure 3. The maximum growth rates $\hat{\omega}_{Im}$ versus Weber number, W, for inviscid jet, viscous jet and viscoelastic jet (2%PO) with $\hat{U} = 1$ and Re= 100.

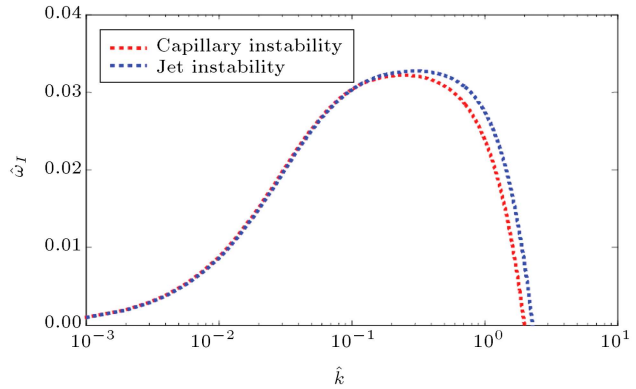

Figure 4. Comparison between the growth rates curves $\hat{\omega}_I$ vs. $\hat{k}$ for viscoelastic jet (2%PAA) and capillary instability.

the same as those obtained by Funada et al. [18]. A viscoelastic liquid jet has a larger growth rate compared to a viscous liquid jet and a smaller growth rate compared to an inviscid liquid jet. The fluid elasticity enhances the growth of instabilities, whereas viscous effects result in a more stable jet. It shows that

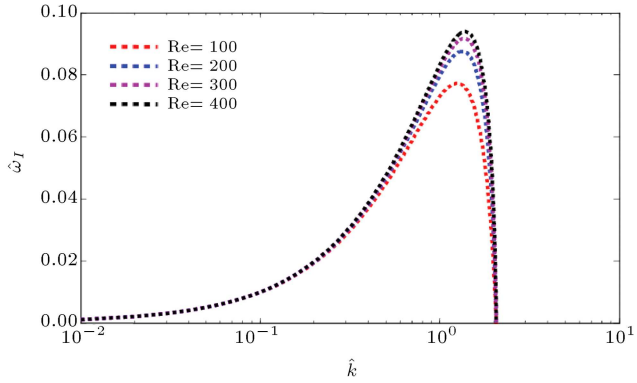

Figure 5. The growth rates curves $\hat{\omega}_I$ vs. $\hat{k}$ for viscoelastic jet (2%PAA) for different values of Reynolds number with $\hat{U} = 1$ and W = 100.

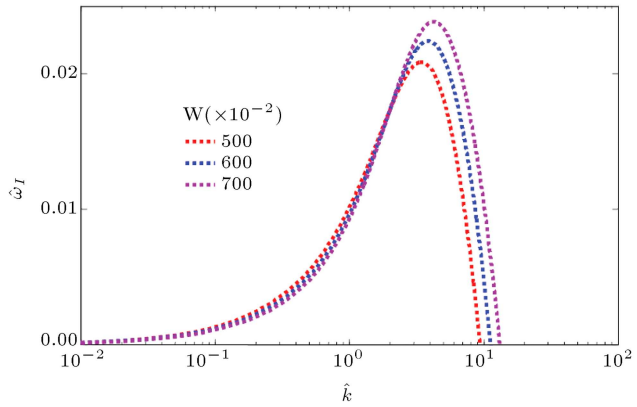

Figure 6. The growth rates curves $\hat{\omega}_I$ vs. $\hat{k}$ for viscoelastic jet (2%PAA) for different values of Weber number with $\hat{U} = 1$ and Re= 100.

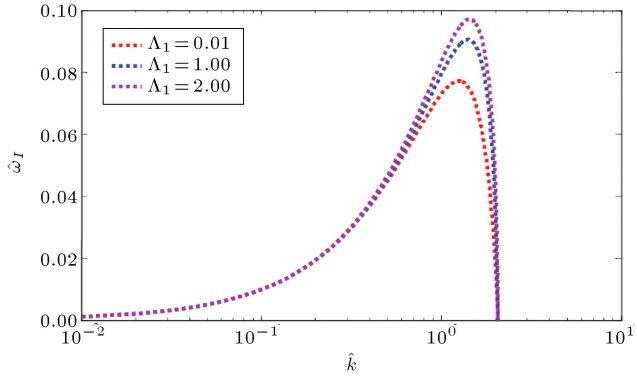

Figure 7. The growth rates curves $\hat{\omega}_I$ vs. $\hat{k}$ for viscoelastic jet (2%PAA) for different values of Deborah number with $\hat{U} = 1$, Re = 100 and W = 100.

viscoelastic jets are more unstable than viscous jets and more stable than inviscid liquid jets. In Figure 3, the maximum growth rate curves for the viscoelastic potential flow of cylindrical jets, the viscous potential flow of liquid and inviscid jets have been compared. In this case, the viscoelastic fluid of Maxwell type (2% Propylene Oxide, PO) has been taken. The result is

Table 2. Comparison of maximum growth rates for different values of W when Re = 100 and $\hat{U} = 1$.

W	Inviscid liquid jet	Viscous liquid jet	Viscoelastic liquid jet (2% PAA)	Viscoelastic liquid jet (2% PO)
1	0.9712	0.8394	0.9430	0.9435
5	0.4348	0.3236	0.4075	0.4077
10	0.3078	0.2093	0.2813	0.2814
50	0.1391	0.0747	0.1152	0.1151
100	0.0996	0.0489	0.0773	0.0771
500	0.0496	0.0204	0.0304	0.0300
1000	0.0406	0.0152	0.0214	0.0208
5000	0.0650	0.0149	0.0209	0.0185
10000	0.1596	0.0195	0.0272	0.0242
50000	0.7981	0.0288	0.0391	0.0355
100000	1.5962	0.0310	0.0414	0.0378
500000	7.9808	0.0328	0.0433	0.0397
1000000	15.9617	0.0330	0.0435	0.0400

Table 3. Comparison of maximum growth rates for different values of Re when and $\hat{U} = 1$.

Re	Inviscid liquid jet	Viscous liquid jet	Viscoelastic liquid jet (2% PAA)	Viscoelastic liquid jet (2% PO)
1	0.3078	0.0282	0.0300	0.0300
10	0.3078	0.1114	0.1586	0.1588
100	0.3078	0.2093	0.2813	0.2814
1000	0.3078	0.2933	0.3054	0.3053
10000	0.3078	0.3063	0.3080	0.3079
100000	0.3078	0.3077	0.3083	0.3082

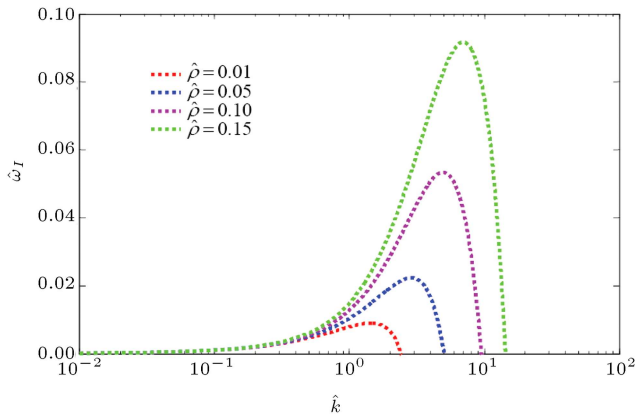

Figure 8. The growth rates curves $\hat{\omega}_I$ vs. $\hat{k}$ for viscoelastic jet (2%PAA) for different values of density ratio with $\hat{U} = 1$, Re = 100 and W = 100.

similar to the previous case, although the growth rate curve is different.

The peak values of maximum growth rates for inviscid liquid jet, viscous liquid jet, cylindrical jet of viscoelastic fluid (2% PAA) and cylindrical jet of viscoelastic fluid (2% PO), for different values of Weber number, are given in Table 2. From Table 2 it is noticed that the peak values for viscoelastic jets (both 2% PAA and 2% PO) are larger in comparison with the peak values of viscous jets and smaller with the peak values of growth rates in inviscid jets. In Table 3, we have compared the maximum growth rates for inviscid jet, viscous jet and viscoelastic jets (both 2%PAA and 2%PO) for different values of Reynolds number, and observed that Reynolds number has a destabilizing effect on the stability of both viscous and viscoelastic jets. Funada and Joseph [17] have done the viscoelastic potential flow analysis of capillary instability. They concluded that the capillary collapse of viscoelastic threads is controlled by two parameters, a Reynolds number and a Deborah number. The density and viscosity ratios are small and only have a small effect. In Figure 4, a comparison between growth rate curves for the capillary instability of viscoelastic fluid and viscoelastic jets has been made. At small wave number, the growth rate for capillary instability is more than the growth rate for a viscoelastic jet, and, at large wave number, the growth rate for capillary instability is less than the growth rate for a viscoelastic jet.

This indicates that at small wave number, capillary instability dominates, while at large wave number, Kelvin-Helmholtz instability dominates.

The evolution of the growth rate curves for different values of Reynolds number is shown in Figure 5. The growth rate is increasing on increasing the value of Reynolds number. Through increasing Reynolds number, the jet viscosity decreases and this clearly shows that jet viscosity can dampen the instability of viscoelastic liquid jets. Also, if the jet velocity increases, the inertia force increases, resulting in increases in the Reynolds number. Therefore, it is concluded that jet velocity influences the instability behaviour. Figure 6 shows that as the Weber number increases, the growth rate also increases for the same value of Reynolds number. The Weber number is inversely proportional to the jet surface tension. As jet surface tension decreases, the growth of the disturbances increases. Therefore, it is concluded that the effect of jet surface tension resists the occurrence and development of instability.

In Figure 7, the growth rate curves for different values of Deborah number, Λ_1, are illustrated. It has been observed that the Deborah number enhances the wave growth rate of disturbances on viscoelastic liquid jets. Hence, it is concluded that the relaxation time of a viscoelastic fluid has a destabilizing effect on the stability of the jet. Variations of the growth rate curves for the different values of density ratio have been shown in Figure 8. It indicates that upon increasing the density of outside fluid, the growth rate increases. It clearly shows that denser outside fluid may destabilize the viscoelastic jets.

Figure 9 compares the growth rate curves for viscoelastic liquid jets for axisymmetric and asymmetric disturbances for different values of Weber number. It has been noticed that at low Weber number, the growth rate curve for asymmetric disturbances is lower in comparison with the curves obtained for axisymmetric disturbances. This concludes that asymmetric disturbances are more stable than axisymmetric disturbances. As Weber number increases, the difference between growth rates for axisymmetric and asymmetric disturbances decreases, but, still, asymmetric disturbances are more stable.

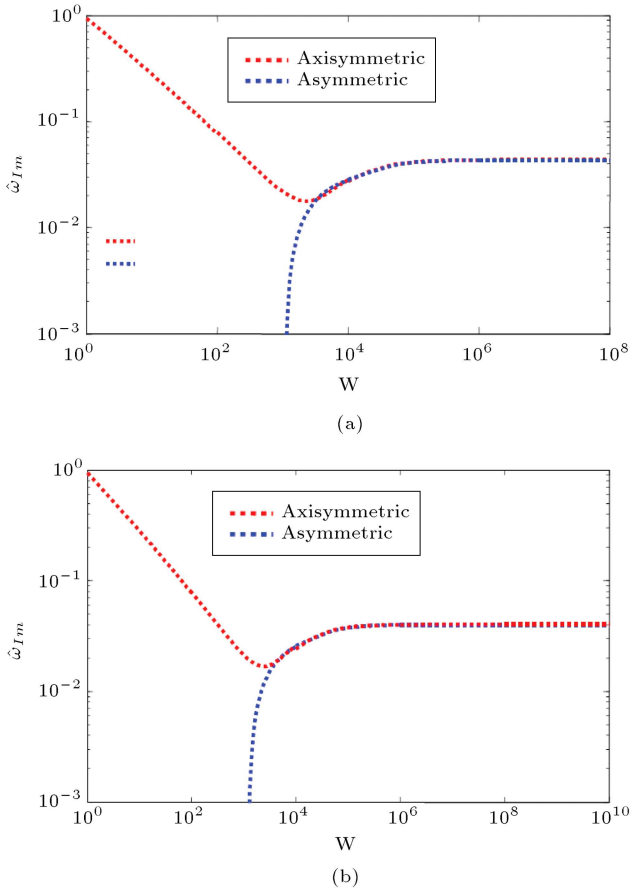

Figure 9. Comparison of maximum growth rates $\hat{\omega}_{Im}$ vs. W for axisymmetric disturbances and asymmetric disturbances with $\hat{U} = 1$ and $\mathrm{Re} = 100$: (a) Viscoelastic Jet (2%PAA); and (b) viscoelastic Jet (2%PO).

6. Conclusion

In the present paper, we have studied the temporal instability behaviour of a viscoelastic cylindrical jet with both axisymmetric and asymmetric disturbances in an infinite viscous fluid, using the concept of potential flow theory. A cubic dispersion relation has been derived and solved. The effect of various physical parameters such as Weber number, Reynolds number and Deborah number etc. has been depicted through various figures. A comparison between inviscid liquid jet, viscous jet and viscoelastic potential flow analysis for cylindrical jets has been made. It has been observed that viscoelastic jets are stable in comparison to inviscid jets, but are unstable in comparison to viscous jets. Weber number, Reynolds number and Deborah number are key measures that affect the stability of the viscoelastic jets. Axisymmetric jets are more unstable than asymmetric viscoelastic jets.

Acknowledgement

One of the authors (M.K.A.) is grateful to the Council of Scientific and Industrial Research (CSIR), New Delhi, for financial support during this work.

Nomenclature

$\mu^{(1)}$	Viscosity of viscoelastic jet
$\rho^{(1)}$	Density of viscoelastic jet
$\mu^{(2)}$	Viscosity of outside viscous fluid
$\rho^{(2)}$	Density of outside viscous fluid

U	Velocity of viscoelastic jet
R	Initial radius of viscoelastic jet
λ_1	Relaxation time of viscoelastic jet
λ_2	Retardation time of viscoelastic jet
σ	Surface tension at the interface
η	Perturbation from equilibrium position
n	Unit outward normal to the interface
$\phi(r,\theta,z,t)$	Velocity potential
k	Wave number
ω	Growth rate

References

1. Rayleigh, L. "On the capillary phenomenon of jets", *Proc. Roy. Soc.*, London A, **29**, pp. 71-97 (1897).
2. Chandrasekhar, S., *Hydrodynamic and Hydromagnetic Stability*, Dover publications, New York (1981).
3. Rayleigh, L. "On the instability of a cylinder of viscous liquid under capillary force", *Philos. Mag.*, **34**, pp. 145-154 (1892).
4. Weber, C. "Zum Zerfall eines Flussigkeitsstrahles. Ztshr. angew", *Math. And Mech.*, **11**, pp. 136-154 (1931).
5. Middleman, S. "Stability of a viscoelastic jet", *Chem. Eng. Sci.*, **20**, pp. 1037-1040 (1965).
6. Goldin, M., Yerushalmi, J., Pfeffer, R. and Shinaar, R. "Breakup of laminar capillary jet of viscoelastic fluid", *J. Fluid Mech.*, **38**, pp. 689-711 (1969).
7. Chang, H.C., Demekhin, E.A. and Kalaidin, E. "Interated stretching of viscoelastic jets", *Phy. Fluids.*, **11**(7), pp. 1717-1737 (1986).
8. Bousfield, D.W., Keunings R., Marruci, G. and Denn, M.M. "Nonlinear analysis of surface driven breakup of viscoelastic filaments", *J. Non-Newtonian Fluid Mech.*, **21**, pp. 79-97 (1986).
9. Brenn, G., Liu, Z. and Durst, F. "Linear analysis of temporal instability of axisymmetrical non-Newtonian liquid jets", *Int. J. Multiphase flow*, **26**, pp. 1621-1644 (2000).
10. Liu, Z. and Liu, Z. "Linear analysis of three-dimensional instability of non-Newtonian liquid jets", *J. Fluid Mech.*, **559**, pp. 451-459 (2006).
11. Liu, Z. and Liu, Z. "Instability of viscoelastic liquid jet with axisymmetric and asymmetric disturbances", *Int. J. Multiphase flow*, **34**, pp. 42-60 (2008).
12. Joseph, D.D. and Liao, T. "Potential flows of viscous and viscoelastic fluids", *J. Fluid Mechanics*, **256**, pp. 1-23 (1994).
13. Funada, T. and Joseph, D.D. "Viscous potential flow analysis of Kelvin-Helmholtz instability in a channel", *J. Fluid Mech.*, **445**, pp. 263-283 (2001).
14. Joseph, D.D., Belanger, J. and Beavers, G.S. "Breakup of a liquid drop suddenly exposed to a high-speed airstream", *Inter. J. Multiphase flow*, **25**, pp. 1263-1303 (1999).
15. Joseph, D.D., Beavers, G.S. and Funada, T. "Rayleigh-Taylor instability of viscoelastic drops at high weber numbers", *J. Fluid Mechanics*, **453**, pp. 109-132 (2002).
16. Funada, T. and Joseph, D.D. "Viscous potential flow analysis of capillary instability", *Inter. J. Multiphase flow*, **28**, pp. 1459-1478 (2002).
17. Funada, T. and Joseph, D.D. "Viscoelastic potential flow analysis of capillary instability", *J. Non-Newtonian fluid mechanics*, **111**(2003), pp. 87-105 (2003).
18. Funada, T., Joseph, D.D. and Yamashita, S. "Stability of liquid jet into incompressible gases and liquids", *Int. J. Multi. Flow*, **30**, pp. 1177-1208 (2004).

Biographies

Mukesh Kumar Awasthi obtained his M.Sc. degree in Mathematics from the University of Lucknow, India, in 2007, and his PhD degree in Mathematics from the Indian Institute of Technology, Roorkee, India, in 2012. Currently, he is working as Assistant Professor in the Department of Mathematics at the University of Petroleum and Energy Studies, Dehradun, India.

Rishi Asthana obtained his M.Sc. degree in Mathematics from Banaras Hindu University, in 2001, and his PhD degree in Mathematics from the Indian Institute of Technology, Roorkee, India, in 2009. Currently, he is working as Assistant Professor in the Department of Mathematics at Galgotia University, Greater Noida, India.

Gopal Saran Agrawal obtained his PhD degree from the Indian Institute of Technology, Kanpur, India, in 1970. Subsequently, he joined the Indian Institute of Technology, Roorkee, where he served as Lecturer, Reader Assistant and Associate Professor in the Department of Mathematics. Currently, he is COE and Head of the Institute of Computer Applications, Manglayatan, India.